

# Microstructures and Properties of Laser-Glazed Plasma-Sprayed $ZrO_2$ - $YO_{1.5}$ /Ni-22Cr-10Al-1Y Thermal Barrier Coatings

H.L. Tsai and P.C. Tsai

Thermal barrier coatings (TBCs) consisting of two layers with various yttria contents ( $ZrO_2$ - $YO_{1.5}$ /Ni-22Cr-10Al-1Y) were plasma sprayed, and parts of the various specimens were glazed by using a pulsed  $CO_2$  laser. All the specimens were then subjected to furnace thermal cycling tests at 1100 °C; the effect of laser glazing on the durability and failure mechanism of the TBCs was then evaluated. From these results, two models were developed to show the failure mechanism of as-sprayed and laser-glazed TBCs: model A, which is thermal-stress dominant, and model V, which is oxidation-stress dominant. For top coats containing cubic phase, cubic and monoclinic phases, or tetragonal and a relatively larger amount of monoclinic phases, whose degradation is thermal-stress dominant, laser glazing improved the durability of TBCs by a factor of about two to six. Segmented cracks that occurred during glazing proved beneficial for accommodating thermal stress and raising the tolerance to oxidation, which resulted in a higher durability. Thermal barrier coatings with top coats containing tetragonal phase had the highest durability. Degradation of such TBCs resulted mainly from oxidation of the bond coats. For top coats with a greater amount of monoclinic phase, thermal mismatch stress occurred during cooling and detrimentally affected durability.

## Keywords

durability, failure analysis, fractograph, laser glazing, microstructure, phase analysis, plasma spraying, thermal barrier coatings, thermal cycling test, yttria-stabilized zirconia

## 1. Introduction

PLASMA-SPRAYED, duplex,  $ZrO_2$ - $YO_{1.5}$ /MCrAlY thermal barrier coatings (TBCs) have been used to insulate air-cooled components in gas turbine engines for many years (Ref 1, 2). Some of the research on TBCs has involved improvements in deposition techniques (Ref 3-5) and materials selection (Ref 6-8). Other efforts have focused on the degradation mechanisms of TBCs (Ref 9-14). Operationally induced stresses and oxidation of the bond coats were identified as the major influences on the degradation of TBCs by several researchers (Ref 6, 9-15). Work by Ruckle (Ref 16) and by Grot and Martyn (Ref 17) indicated that the life of as-sprayed TBCs is significantly improved by segmented cracks. Previous research (Ref 18-26) showed that the laser glazing process would produce segmented cracks within the ceramic layer. On the basis of the degradation mechanisms of TBCs and the beneficial effects of segmented cracks, laser glazing was considered a promising process for improving the performance of TBCs.

Although several studies have been conducted on laser glazing of TBCs, many disputes and questions still exist about the effects of laser glazing on TBC durability. It has been shown (Ref 21) that laser-glazed TBCs exhibited an approximate four-fold improvement in life in cyclic oxidation tests compared to as-sprayed TBCs. Results of previous research (Ref 22) also showed that laser glazing enhanced the thermal cyclic life of

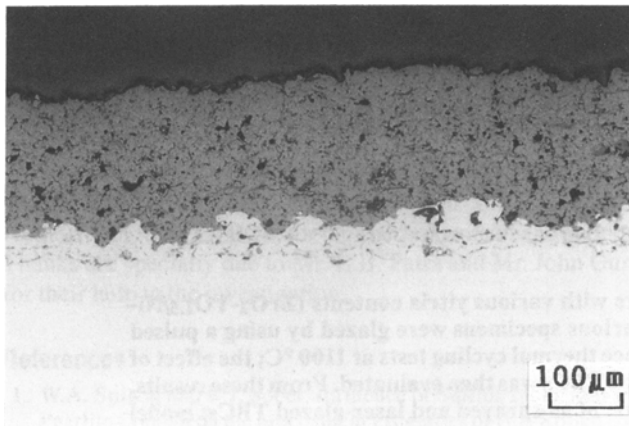
plasma-sprayed TBCs by a factor of about two to six, depending on the heating cycle length and the definition of cyclic life. Effects on life improvement were more pronounced for specimens with a short heating cycle length. Miller and Berndt (Ref 27) also indicated that surface spalling of TBCs due to a high heat flux environment was prevented by laser glazing. Zaplatynsky (Ref 24) reported that laser glazing of TBCs produced a fourfold improvement in life in cyclic hot corrosion tests with a 100 ppm Na fuel equivalent, whereas no apparent effect on their lifetime was observed in cyclic oxidation tests. These inconsistencies may be due to differences in the laser-processing parameters and the materials used.

Previous studies by the authors (Ref 21, 22) were concerned with top coats containing 12 and 19.5 wt% yttria, respectively. Miller et al. (Ref 7) indicated that the most durable coatings were those where the level of yttria is in the range of approximately 6 to 9 mol%  $YO_{1.5}$ . (Compositions expressed throughout in mol% yttria are taken as  $YO_{1.5}$ .) A study by Suhr et al. (Ref 8) showed that the top coat that contained more tetragonal phase and less monoclinic phase exhibited longer cyclic life. In view of this, the cyclic life of TBCs seems to be significantly affected by the yttria content and the phase content. Therefore, it is necessary to identify the cyclic behavior of laser-glazed zirconia-yttria TBCs with various yttria contents.

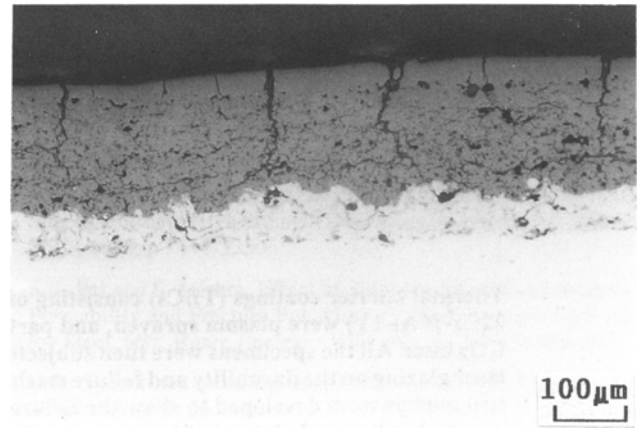
## 2. Experimental Procedure

The substrates, 100 by 25 by 2 mm Hastelloy-X superalloy coupons, were grit blasted with alumina powder and sprayed first with a Ni-22Cr-10Al-1Y bond coat and then with a yttria-stabilized zirconia (YSZ) top coat using an air-plasma spray system. The designed compositions of the top coats and the spraying parameters applied in this study are listed in Table 1. The top coat powder contained 1.6 to 2.1 wt%  $HfO_2$ . All mate-

H. L. Tsai and P.C. Tsai, Department of Mechanical Engineering and Technology, National Taiwan Institute of Technology, Taipei, Taiwan, 10772, R.O.C.



(a)



(b)

Fig. 1 Typical optical microstructure of the cross section of 19.5YSZ TBCs. (a) As-sprayed. (b) As-glazed

Table 1 Plasma spraying parameters

Coating	Particle size, $\mu\text{m}$	Arc current, A	Argon flow rate, L/min	Hydrogen flow rate, L/min	Powder feed rate, g/min	Spray distance, mm	Incident angle, degrees	Incident velocity, m/s
Ni-22Cr-10Al-1Y	...	630	58	11	36	140	90	290
ZrO <sub>2</sub> -6.1wt%YO <sub>1.5</sub>	...	630	42	11	40	120	90	290
ZrO <sub>2</sub> -7.3wt%YO <sub>1.5</sub>	20-75	630	44	13	40	120	90	290
ZrO <sub>2</sub> -12wt%YO <sub>1.5</sub>	20-75	630	44	13	40	120	90	290
ZrO <sub>2</sub> -19.5wt%YO <sub>1.5</sub>	15-90	600	35	10	40	120	90	290

Table 2 Lazer glazing parameters

Power, W	450
Travel speed, mm/min	2000
Pulse, Hz	800
Duty, %	20
Melting width, mm	12
Overlap, mm	1
Energy density, J/mm <sup>2</sup>	0.225
Melting depth, $\mu\text{m}$	36

rials were obtained from a single vendor. The thicknesses of the top coat and the bond coat were about 220  $\mu\text{m}$ , respectively. Some as-sprayed specimens were glazed by using a pulsed CO<sub>2</sub> laser with a cylindrical focal lens. The focus was set on the sample surface. The laser glazing parameters are given in Table 2.

Both as-sprayed and glazed specimens were then subjected to a furnace thermal cycling test. Each cycle of the test was 1 h at  $1100 \pm 5$  °C, followed by 10 min of forced-air cooling to ambient temperature outside the furnace. The weights of all specimens were measured every cycle or every other cycle with an analytical-type balance with an accuracy of  $\pm 0.1$  mg. The microstructures of both as-processed and cycled TBCs were investigated with optical microscopy and scanning electron microscopy (SEM). An electron probe microanalyzer (EPMA) was used for analyzing elemental distribution. X-ray diffractometry (XRD) was used to analyze the phases of the oxide and the top coat. The mole ratios of the phases of the top coat were calculated using expressions from Miller et al. (Ref 28).

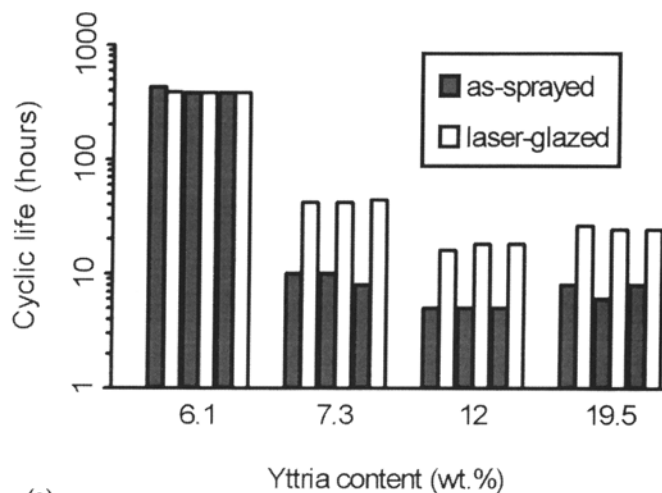
### 3. Results and Discussion

#### 3.1 General Microstructures

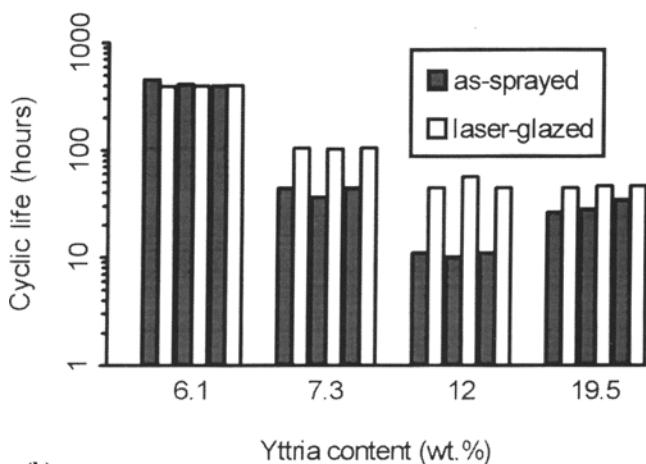
In order to eliminate any effect on durability caused by coating thickness, the thickness of the top coat with varying yttria content was controlled in the range of 200 to 240  $\mu\text{m}$ . The porosity of the top coat was approximately 8 to 15%, and there were no noticeable differences among the specimens. Typical optical microstructures of the as-sprayed and as-glazed coatings are shown in Fig. 1(a) and (b), respectively. The glazed layer had segmented cracks perpendicular to the surface. The melting depth measured in the central portion of the glazed tracks was approximately 36  $\mu\text{m}$ .

#### 3.2 Thermal Cycling Tests

For ease of understanding and description, the TBCs with top coats of 6.1, 7.3, 12, and 19.5 wt% yttria are referred to as 6.1YSZ, 7.3YSZ, 12YSZ, and 19.5YSZ, respectively. Figure 2 shows the cyclic life of different specimens. As shown in Fig. 2(a), the laser-glazed 7.3YSZ, 12YSZ, and 19.5YSZ TBC specimens exhibited a threefold to fourfold improvement in durability on the basis of initial spallation as compared to as-sprayed TBC specimens. Figure 2(b) shows the results of durability on the basis of 50% spallation: The lifetimes of laser-glazed 7.3YSZ, 12YSZ, and 19.5YSZ TBCs varied according to yttria content and were at least twice as durable than their as-sprayed counterparts. For 6.1YSZ TBCs, no improvement in



(a)



(b)

**Fig. 2** Cyclic life of TBCs with various yttria content. (a) On the basis of initial spallation. (b) On the basis of 50% spallation generated on one side

durability occurred after laser glazing, regardless of the initial spallation lifetime or of the 50% spallation lifetime.

Figure 3 shows the maximum weight gain of the specimens. Laser-glazed TBCs endured more weight gain than their as-sprayed counterparts for 7.3YSZ, 12YSZ, and 19.5YSZ just before spallation was initiated. The 6.1YSZ specimen showed no evident difference between the as-sprayed and laser-glazed samples. Regardless of condition, the weight gain of 6.1YSZ specimens was higher than any of the other three specimens.

### 3.3 Phase Analysis of the Top Coat

Phase analysis of the ceramic top coat was performed using XRD. The results are summarized in Table 3. The mole percentage of  $YO_{1.5}$ , which was calculated by  $c/a$  ratio or lattice parameter  $a$ , was 1 to 3 mol% higher than indicated in data supplied by the vendor. In this study, the powder contained 1.6 to 2.1 wt%  $HfO_2$ . Research undertaken by Miller and his colleagues (Ref 7) found no significant difference between the diffraction patterns of as-sprayed  $HfO_2$ -containing grade and

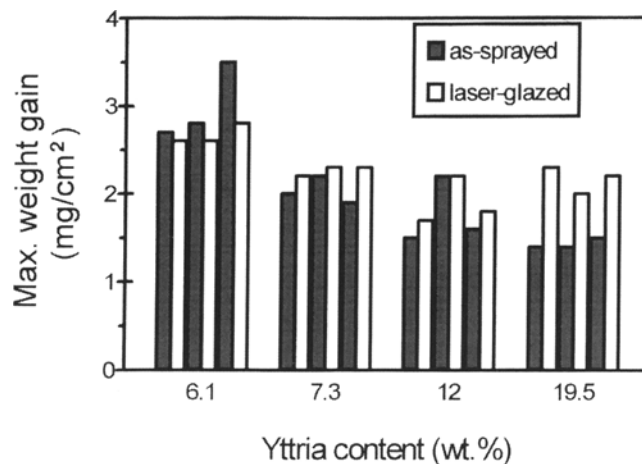


**Fig. 3** Maximum weight gain just before spallation was initiated

those of high-purity  $ZrO_2/9$  mol%  $YO_{1.5}$ . The reason for this is that  $HfO_2$  and  $ZrO_2$  form solid solutions; therefore, the lattice parameter  $a$ , the  $c/a$  ratio, and the  $YO_{1.5}$  content obtained from XRD are reliable.

The phase distribution of the top coat is also shown in Table 3. For the raw powder and sprayed coatings, the mole fractions of the monoclinic phase for 6.1YSZ, 7.3YSZ, and 12YSZ were, respectively, 1, 4, and 12 mol%. The microstructures revealed in the 19.5YSZ sample consisted exclusively of the cubic phase. In addition, XRD analysis of all as-sprayed samples showed no perceptible change after the cyclic tests.

For glazed samples, the XRD analyses showed that the monoclinic phase occurred in none of the specimens. With the exception of 12YSZ, there were no significant differences between as-glazed and glazed specimens after cycling tests. The glazed 12YSZ coatings after 44 cycles at 1100 °C consisted of both cubic and tetragonal phases, while the as-glazed 12YSZ coatings revealed an exclusively cubic phase.

### 3.4 Failure Analysis

Previous studies (Ref 9-15) showed that the major factors causing degradation of TBCs were oxidation of the bond coat and thermal stress, and that (Ref 22) thermal stress and oxidation of the bond coat had a major influence on the degradation of 19.5YSZ TBCs. It has also been shown that in tests with a short heating length for each cycle, degradation was due mainly to thermal stress. The research undertaken in the current paper shows that the failure morphology of 7.3YSZ and 12YSZ coincides with that of 19.5YSZ TBCs. The mechanism for this kind of degradation (hereafter referred to as model A) and its failure morphologies were described in detail in a previous study (Ref 22), where cracks initiated in the ceramic top coat near the top coat/bond coat interface just above the higher asperity and propagated within the top coat. The cracks crossed over the asperity of the bond coat. There was a thin residual ceramic layer attached to the bond coat after the top coat had spalled.

Figure 4 shows optical cross-sectional views of 6.1YSZ TBC after 394 cycles. Cracks initiated for the most part either within the top coat near the valleys of the bond coat (labeled C)

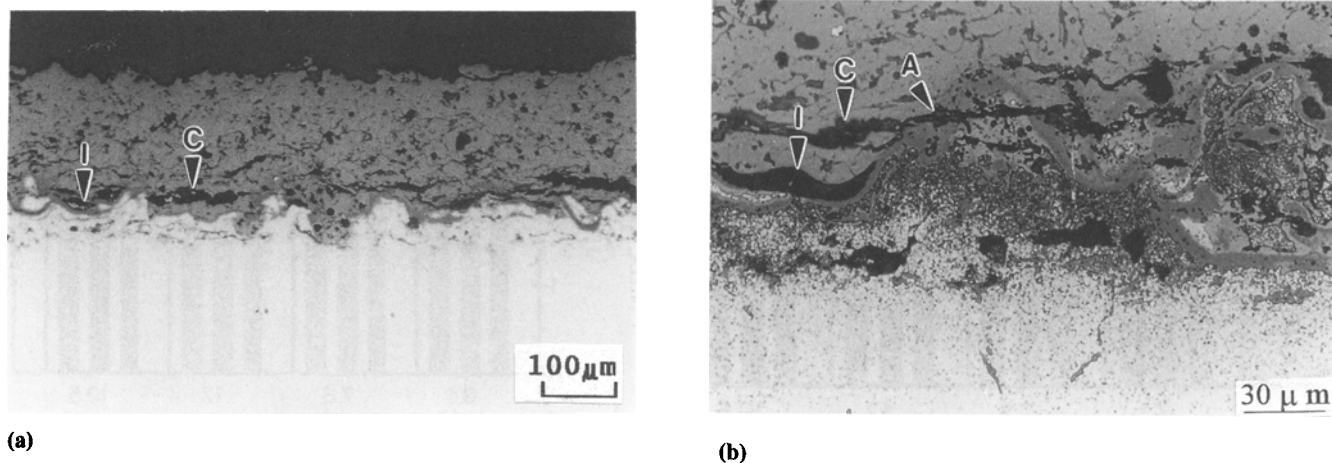


Fig. 4 Cross-sectional optical micrographs of 6.1YSZ TBCs after 394 cycles. (a) As polished. (b) Etched

Table 3 Phase analysis of top coat

YO <sub>1.5</sub> (a), wt % (mol %)	Sample	Phase distribution(b), mol %			YO <sub>1.5</sub> in T', mol %	c/a for T'
		M	F	T'		
6.1 (6.7)	Powder	0	100	[F(c) + T']	7.6	1.0124
	As sprayed	0	100	[F(c) + T']	8.6	1.0112
	Sprayed + 394 cycles	0	100	[F(c) + T']	7.6	1.0124
	As glazed	0	100	[F(c) + T']	8.3	1.0114
	Glazed + 398 cycles	0	100	[F(c) + T']	7.4	1.0126
7.3 (8)	Powder	12	88	[F(c) + T']	10	1.0092
	As sprayed	12	88	[F(c) + T']	11.0	1.0079
	Sprayed + 46 cycles	12	88	[F(c) + T']	10.1	1.0091
	As glazed	0	100	[F(c) + T']	10.1	1.0091
	Glazed + 104 cycles	0	100	[F(c) + T']	9	1.0105
					YO <sub>1.5</sub> in F	a for F
12 (13)	Powder	3	97	0	15.3	5.1352
	As sprayed	4	96	0	14.1	5.1328
	Sprayed + 11 cycles	4	96	0	15.9	5.1364
	As glazed	0	100	0	13.5	5.1316
	Glazed + 44 cycles	0	100	[F + T'(c)]	14.1	5.1328
19.5 (21)	Powder	0	100	0	21.8	5.1484
	As sprayed	0	100	0	22.3	5.1496
	Sprayed + 26 cycles	0	100	0	23.6	5.1556
	As glazed	0	100	0	20.6	5.1460
	Glazed + 44 cycles	0	100	0	21.2	5.1472

(a) Data from vendor. (b) M, monoclinic; F, cubic; T', tetragonal. (c) If present, only a minor amount (less than 5%)

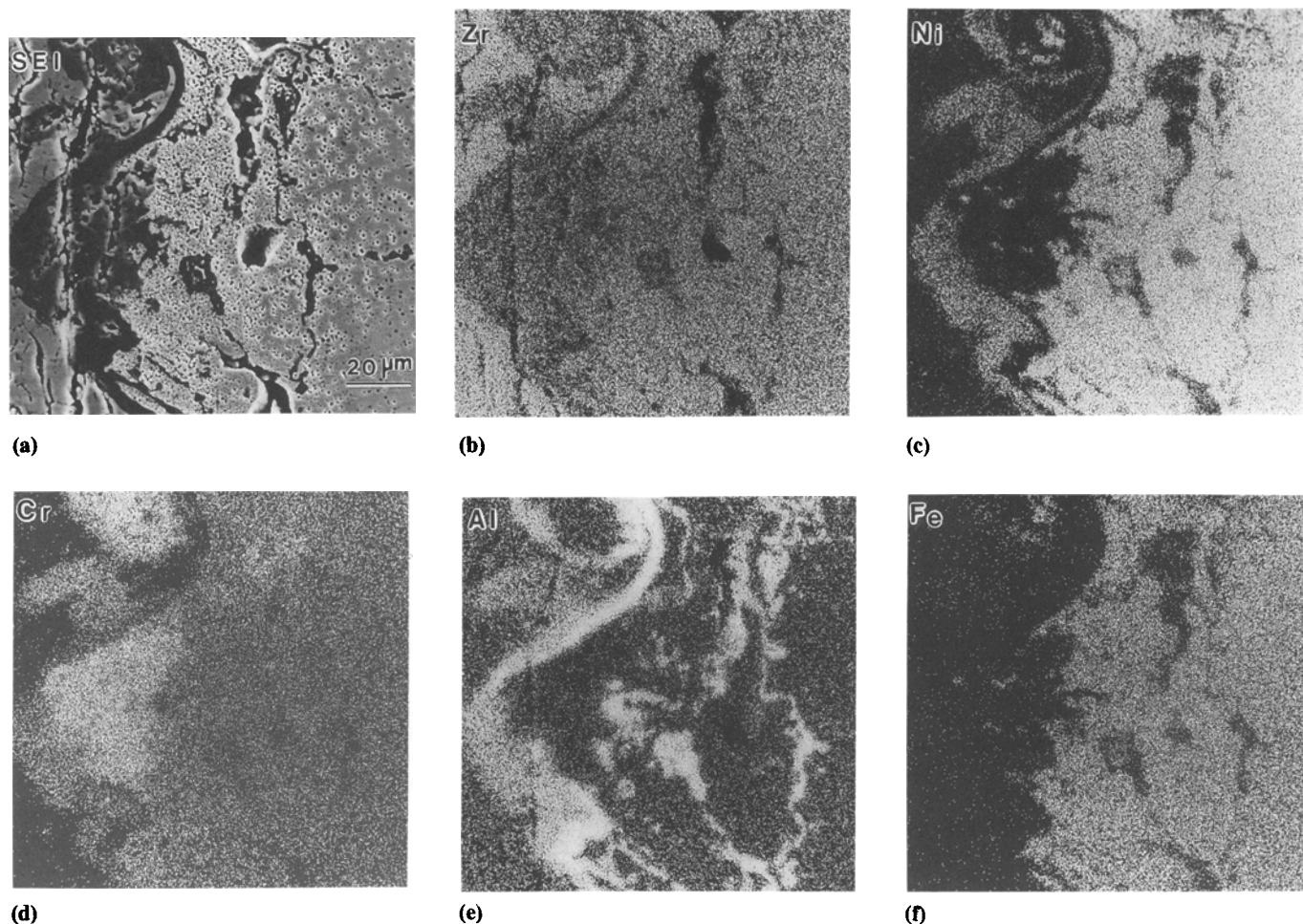
or at the top coat/bond coat interface (labeled I); after propagating in the top coat near the bond coat, the top coat became spalled. The mechanism for such spalling failure shall be referred to as model V. In Fig. 4(b), the label A shows the cracks traversing the oxide scale at the asperity; the spalled oxide scale is attached to the underside of the top coat. An enlargement of this area is given in Fig. 5, which shows the secondary-emission electron image (SEI) microstructure and x-ray mapping.

Figure 6 shows fractographs of the bottom of the spalled top coat for 6.1YSZ. The dark area in Fig. 6(a) indicates the attached oxide, an enlargement of which is shown in Fig. 6(b).

The bottoms of spalled 6.1YSZ and 19.5YSZ top coats were analyzed by XRD. Oxide peaks were found for 6.1YSZ, but not for 19.5YSZ. This implies that a considerable amount of oxide

was attached underneath the spalled 6.1YSZ top coat. The main oxide was NiCr<sub>2</sub>O<sub>4</sub>, and there was a small amount of NiO, but no Cr<sub>2</sub>O<sub>3</sub> was detectable. This clearly indicates the mechanism for degradation of the 6.1YSZ TBCs, in which cracks propagate along the oxide scale or within the top coat.

Research by Chang et al. (Ref 29, 30) shows that, owing to a difference in thermal expansion, thermal stress occurs within the top coat near the asperity of the bond coat, which is tensile stress running perpendicular to the top coat. When oxidation occurs near the valleys of the bond coat, tensile stress running perpendicular to the top coat also occurs. This verifies the crucial role that thermal stress plays in the degradation of 7.3YSZ, 12YSZ, and 19.5YSZ TBCs; moreover, it reinforces the deduction that the degradation of 6.1YSZ TBC is due to oxidation stress rather than to thermal stress.



**Fig. 5** Secondary-emission electron image (a) and x-ray mapping of zirconium (b), nickel (c), chromium (d), aluminum (e), and iron (f) for 6.1YSZ TBCs after 394 cycles

### 3.5 Mechanisms by Which Laser Glazing Improves Durability

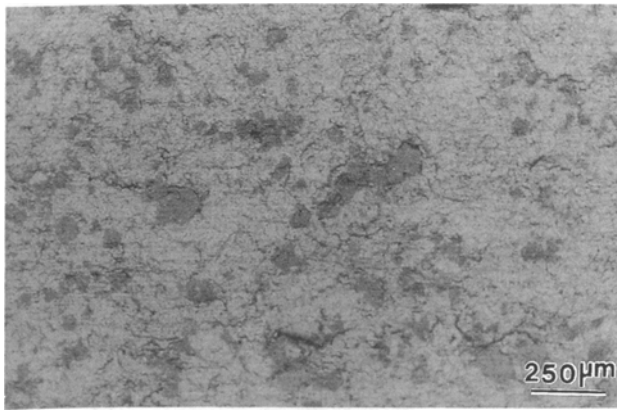
As stated in section 3.2, 6.1YSZ TBC had the highest durability, but this was completely unaffected by laser glazing. The other three TBCs (7.3YSZ, 12YSZ, and 19.5YSZ), however, all showed a marked improvement after the laser glazing process; even so, their highest cycles were not comparable to those for 6.1YSZ.

Figure 7 is a comparison of oxidation rates for the as-sprayed TBCs. It can be seen that the lowest rate is for 19.5YSZ TBC, and its durability is also lower than 6.1YSZ and 7.3YSZ TBCs. Although the oxidation rates for the other specimens (6.1YSZ, 7.3YSZ, and 12YSZ) were very similar, their levels of durability were noticeably different. It is thus apparent that the durability of TBCs is not influenced by variations in the oxidation rate.

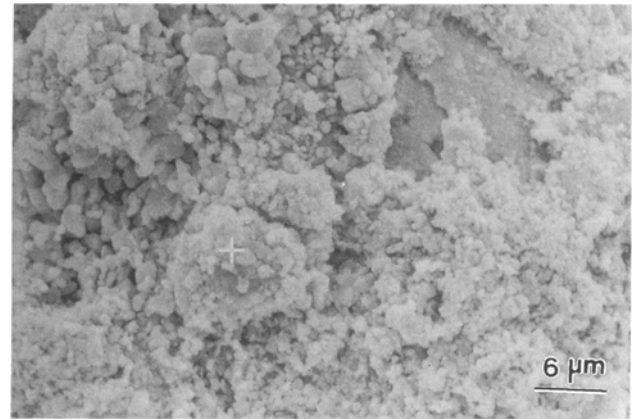
Other research (Ref 31) has shown that the tetragonal phase contains many domain structures. The fracture toughness of tetragonal phase material is two to three times that of cubic phase materials. In the present work, it has been found that the durability of TBCs consisting largely of tetragonal phase (i.e., 6.1YSZ and 7.3YSZ) is higher than that of TBCs with cubic phase (i.e., 12YSZ and 19.5YSZ).

Figure 2 shows that the cyclic life of 12YSZ, containing cubic and monoclinic phases, is lower than that of 19.5YSZ, which contained only a cubic phase. Although 6.1YSZ and 7.3YSZ both consisted of tetragonal and monoclinic phases, the amount of the monoclinic phase of 7.3YSZ was greater than that of 6.1YSZ (12 and 1 mol%, respectively). It is thus no surprise that the durability of 7.3YSZ is lower than that of 6.1YSZ, which confirms that the monoclinic phase has an adverse effect on the durability of TBCs.

Work done by Miller et al. (Ref 7) and Suhr et al. (Ref 8) showed that TBCs having top coats with high amounts of tetragonal phase and low amounts of monoclinic phase had the greatest durability. Miller et al. surmised that a small amount of monoclinic phase in top coats could prolong durability. They also thought that the martensitic transformation of the high-temperature cubic phase on cooling may produce a favorable microcrack network in a top coat. This network could then dissipate energy associated with the extension of large cracks and thus have a positive effect on the durability of TBCs. The top coats studied by Miller and coworkers consisted mostly of tetragonal phase with some monoclinic phase, which ranged from 8 to 40 mol%; the cyclic life was from 400 to 620 cycles. It is thus obvious that under these conditions, the monoclinic phase has no real effect on durability.



(a)



(b)

**Fig. 6** SEM fractographs of the bottom of the 6.1YSZ top coat after 394 cycles. (a) Backscattered-electron image. (b) Higher magnification of the dark area in (a), SEI

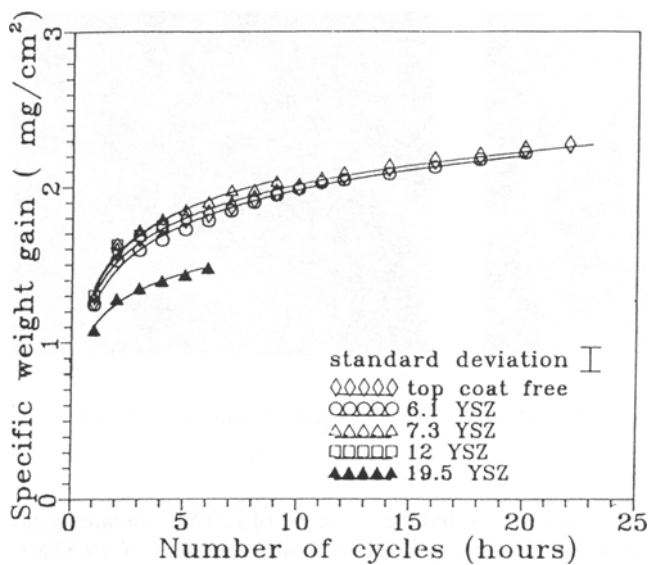


**Fig. 7** Relationship between specific weight gain and accumulating cycles for as-sprayed TBCs with various yttria contents

In the study by Suhr et al., the amount of monoclinic phase ranged from 8 to 22 mol%, and durability increased as the amount of monoclinic phase decreased. As shown in Fig. 2, the durability of as-sprayed 6.1YSZ TBCs was 400 cycles, while that of the 7.3YSZ TBCs was a mere 10 cycles. As 6.1YSZ contained 1 mol%, and 7.3YSZ, 12 mol%, it is apparent that a top coat containing monoclinic phase has a detrimental effect on durability; likewise, a beneficial effect is achieved when a top coat contains a higher amount of tetragonal phase.

For 7.3YSZ and 12YSZ TBCs, the glazed layer contained no monoclinic phase; however, an as-sprayed layer existed between the bond coat and the glazed layer. This lack of a monoclinic phase in the glazed layer clearly, then, is not a factor in increasing durability. Moreover, the as-sprayed 19.5YSZ TBC contained no monoclinic phase, but rather consisted exclusively of cubic phase. Laser glazing improved the durability of 19.5YSZ TBC. As discussed, the degradation of 7.3YSZ, 12YSZ, and 19.5YSZ TBC specimens results mainly from the

**Table 4** Thickness of oxide scale on failed specimens and failure model

Sample	Maximum weight gain, mg/cm <sup>2</sup>	Thickness of oxide scale, μm	Failure model
6.1YSZ	3.00(a)	7.8	V
7.3YSZ	2.03	3.7	A
12YSZ	1.76	2.3	A
19.5YSZ	1.43	3.2	A

(a) Calculated for 100 cycles

effects of thermal and oxidation stress. Likewise, it has been shown that the laser glazing process has a positive effect on the durability of such specimens. Of even greater significance is that this proves that the greatest factor affecting the durability of laser-glazed TBCs is the segmented cracks that traverse the surface. These cracks are obviously conducive to relieving stress and raising the strain tolerance of the top coat.

The effects of strain tolerance on the stress of TBCs can be seen more clearly by an analysis of the stress-strain curve of ceramic coatings. Measurements by Shi et al. (Ref 32) of the mechanical properties of sprayed ceramic coatings showed that the typical stress-strain curve for this type of coating was non-linear and could be expressed by:

$$\epsilon = \epsilon^e + \epsilon^{ne} \quad (\text{Eq 1})$$

where  $\epsilon^e$  represents

$$\epsilon^e = \frac{\sigma}{E} \quad (\text{Eq 2})$$

which is the nominal strain and is estimated on the basis of linear elastic behavior, and where  $\epsilon^{ne}$  represents the inelastic strain resulting from laminar and microcrack structures. This study also showed that the fracture strain of the ceramic coatings increased with a decrease in coating thickness. In general, there is no evident difference in nominal strain among the same



materials. Therefore, increases in fracture strain could be expected from increases in inelastic strain.

After the laser glazing of TBCs, between the glazed layer and the bond coat is a nonsegmented as-sprayed layer that is thinner than the top coat. Therefore, the laser glazing process should increase the strain tolerance of the top coat. Likewise, the total strain ( $\epsilon$ ) of the top coat also increases with the presence of inelastic strain ( $\epsilon^{ne}$ ) and results in a reduction of the Young's modulus. For this reason, the thermal mismatch stress is reduced. These same results were achieved by Chang et al. (Ref 30) using the finite-element method. A reduction in thermal stress facilitates an improvement in the durability of TBCs. For the 6.1YSZ TBCs studied in this paper, degradation resulted mainly from oxidation stress; thus, laser glazing had no effect on improving their durability.

In order to better understand the effect of the thickness of an oxide scale on the degradation of TBCs, measurements of the oxide scale on as-sprayed TBCs of various compositions were made after cyclic testing. Using optic photographs, the thickness of the oxide scale was measured near the valleys of the bond coat. These measurements, along with a failure model, are listed in Table 4. The oxide thickness for 7.3YSZ, 12YSZ, and 19.5YSZ is 3.7, 2.3, and 3.2  $\mu\text{m}$ , respectively; the failure model for these specimens is model A.

The results of two other studies were utilized to further explain why 7.3YSZ, 12YSZ, and 19.5YSZ TBCs failed. In the first study, by Chang and Phucharoen (Ref 29), it was shown that an oxide with a thickness of 3  $\mu\text{m}$  produced about 12 MPa oxidation stress. In the second study, by Shankar et al. (Ref 33), it was found that the strength of as-sprayed  $\text{ZrO}_2$ -8 wt%  $\text{Y}_2\text{O}_3$  coatings was 30.5 to 39.8 MPa. As 12 MPa stress is obviously much lower than 30.5 MPa, this level of stress could not result in failure of TBCs. The only other plausible explanation for the failure of the 7.3YSZ, 12YSZ, and 19.5YSZ TBCs is thermal stress. The oxide scale of 6.1YSZ TBCs was 7.8  $\mu\text{m}$  thick. Assuming that the oxidation stress is in proportion to the thickness of the oxide scale, then, on the basis of the Chang study just mentioned, the oxidation stress should be 31 MPa; thus, the stress of such a coating would fall within the range of 30.5 to 39.8 MPa reported by Shankar et al. Other research (Ref 34) has verified that both heat treatment and oxidation of the bond coat affected the reduction in strength of TBCs. Therefore, an oxidation stress of 31 MPa easily results in failure. These facts thus prove that the degradation of 6.1YSZ TBCs was due to oxidation of the bond coat.

#### 4. Conclusions

For top coats containing cubic phase, cubic and monoclinic phases, or tetragonal phase and a relatively larger amount of monoclinic phase (that is, coating with a yttria content in the range of 7.3 to 20 wt%), laser glazing improved the durability of TBCs by a factor of about two to six, depending on yttria content and the definition of cyclic life.

Thermal barrier coatings whose top coats contain tetragonal phase and minor amounts of monoclinic phase (approximately 1 mol%) have the highest durability. The degradation of such TBCs results mainly from oxidation of the bond coat, and the laser glazing process does not significantly improve durability.

Two models can show the mechanism for degradation of the as-sprayed and laser-glazed TBCs: model A, which is thermal-stress dominant, and model V, which is oxidation-stress dominant. Thermal barrier coatings whose degradation is thermal-stress dominant show an improvement with laser glazing.

#### Acknowledgments

Financial support from the National Science Council (No. NSC 81-0405-E-011-06) of the Republic of China (Taiwan) is acknowledged. The authors would also like to express their appreciation to Dr. David C. Tu, vice president of Mooney Company Ltd., Taipei, for his kind assistance.

#### References

1. P. Vincenzini, Zirconia Thermal Barrier Coatings for Engine Applications, *Ind. Ceram.*, Vol 10 (No. 3), 1990, p 113-126
2. W.J. Lackey, D.P. Stinton, G.A. Cerny, A.C. Schaffhauser, and L.L. Fehrenbacher, Ceramic Coatings for Advanced Heat Engines—A Review and Projection, *Adv. Ceram. Mater.*, Vol 2 (No. 1), 1987, p 24-30
3. S.B. Qadri, E.F. Skelton, C. Kim, M.Z. Harford, and P. Lubitz, Electron-Beam Deposition of Zirconia Films Stabilized in High Temperature Phases by Different Oxides, *Surf. Coat. Technol.*, Vol 49, 1991, p 67-70
4. D.J. Wortman, B.A. Nagaraj, and E.C. Duderstadt, Thermal Barrier Coatings for Gas Turbine Use, *Mater. Sci. Eng.*, Vol A121, 1989, p 433-440
5. H. Herman and N.R. Shankar, Survivability of Thermal Barrier Coatings, *Mater. Sci. Eng.*, Vol 88, 1987, p 69-74
6. F. Vasiliu, I. Pencea, V. Manoliu, I. Dinca, and C. Sarbu, Thermal Stability of Plasma-Sprayed Zirconia Coatings as Related to Substrate Selection, *Am. Ceram. Soc. Bull.*, Vol 64 (No. 3), 1985, p 1268-1271
7. R.A. Miller, R.G. Garick, and J.L. Smialek, Phase Distribution in Plasma Sprayed Zirconia-Yttria, *Am. Ceram. Soc. Bull.*, Vol 62 (No. 3), 1983, p 1355-1358
8. D.S. Suhr, T.E. Mitchell, and R.J. Keller, Microstructure Durability of Zirconia Thermal Barrier Coatings, *Advances in Ceramics*, Vol 12, N. Claussen and A.H. Heuer, Ed., American Ceramic Society, 1984, p 503-517
9. R.A. Miller and C.E. Lowell, Failure Mechanisms of Thermal Barrier Coatings Exposed to Elevated Temperatures, *Thin Solid Films*, Vol 95, 1982, p 265-273
10. C.C. Berndt and H. Herman, Failure during Thermal Cycling of Plasma-Sprayed Thermal Barrier Coatings, *Thin Solid Films*, Vol 108, 1983, p 427-437
11. A. Bennett, Properties of Thermal Barrier Coatings, *Mater. Sci. Technol.*, Vol 2 (No. 5), 1986, p 257-261
12. B.C. Wu, E. Chang, S.F. Chang, and D. Tu, Degradation Mechanisms of  $\text{ZrO}_2$ -8wt%  $\text{Y}_2\text{O}_3$ -22Cr-10Al-1Y Thermal Barrier Coatings, *J. Am. Ceram. Soc.*, Vol 72 (No. 2), 1989, p 212-218
13. B.C. Wu, E. Chang, C.H. Chao, and M.L. Tsai, The Oxide Pegging Spalling Mechanism and Spalling Modes of  $\text{ZrO}_2$ -8wt%  $\text{Y}_2\text{O}_3$ /Ni-22Cr-10Al-1Y Thermal Barrier Coatings under Various Operating Conditions, *J. Mater. Sci.*, Vol 25, 1990, p 1112-1119
14. S. Stecura, Two-Layer Thermal Barrier Coating for High Temperature Components, *Am. Ceram. Soc. Bull.*, Vol 56 (No. 12), 1977, p 1082-1086
15. R.D. Maier, C.M. Scheuermann, and C.W. Andrews, Degradation of a Two-Layer Thermal Barrier Coating under Thermal Cycling, *Am. Ceram. Soc. Bull.*, Vol 60 (No. 5), 1981, p 555-560

16. D.L. Ruckle, Plasma-Sprayed Ceramic Thermal Barrier Coatings for Turbine Vane Platforms, *Thin Solid Films*, Vol 73, 1980, p 455-461
17. A.S. Grot and J.K. Martyn, Behavior of Plasma-Sprayed Ceramic Thermal-Barrier Coatings for Gas Turbine Applications, *Am. Ceram. Soc. Bull.*, Vol 60 (No. 8), 1981, p 807-811
18. P.C. Tsai, H.L. Tsai, and D.C. Tu, Effect of Processing Parameters on Laser Glazing of Plasma Sprayed Yttria Stabilized Zirconia, *Laser Advanced Materials Processing LAMP '92*, A. Matsunawa and S. Katayama, Ed., High Temperature Society of Japan, 1992
19. H.L. Tsai, P.C. Tsai, and D.C. Tu, Characterization of Laser Glazed Plasma Sprayed Yttria Stabilized Zirconia Coatings, *Mater. Sci. Eng.*, Vol A161, 1993, p 145-155
20. P.C. Tsai, H.L. Tsai, and D.C. Tu, Study of Processing Variables in Laser Glazing Plasma-Sprayed Thermal Barrier Coatings, *Mater. Sci. Eng.*, Vol A165, 1993, p 167-173
21. P.C. Tsai, H.L. Tsai, and D. C. Tu, Laser Glazing of Plasma Sprayed Thermal Barrier Coating and Its Effect on High Temperature Cyclic Oxidation Behaviour, *Proc. 1992 Annual Conf. Chinese Society for Materials Science*, Chinese Society for Materials Science, 1992
22. H.L. Tsai and P.C. Tsai, Thermal Cyclic Response of Laser-Glazed Plasma-Sprayed  $ZrO_2$ -19.5wt% $Y_2O_3$ /Ni-22Cr-10Al-1Y Thermal Barrier Coatings, *Mater. Sci. Eng.*, Vol A177, 1994, p 227-232
23. N. Iwamoto, N. Vmesaki, Y. Katayama, and H. Kuroki, Surface Treatment of Plasma-Sprayed Ceramic Coatings by a Laser Beam, *Surf. Coat. Technol.*, Vol 34, 1988, p 59-67
24. I. Zaplatynsky, Performance of Laser-Glazed Zirconia Thermal Barrier Coatings in Cyclic Oxidation and Corrosion Burner Rig Tests, *Thin Solid Films*, Vol 95, 1982, p 275-284
25. R. Sivakumar and B.L. Mordike, Laser Melting of Plasma Sprayed Ceramic Coatings, *Surf. Eng.*, Vol 4 (No. 2), 1988, p 127-140
26. M. Havrda, K. Volrník, J. Wagner, and P. Mráz, Laser Treatment of Plasma Sprayed Zirconium Silicate Coating, *Advances in Thermal Spraying ITSC '86*, Welding Institute of Canada, Pergamon Press, 1986, p 569-575
27. R.A. Miller and C.C. Berndt, Performance of Thermal Barrier Coatings in High Heat Flux Environments, *Thin Solid Films*, Vol 119, 1984, p 195-202
28. R.A. Miller, J.L. Smialek, and R.G. Garick, Phase Stability in Plasma-Sprayed Partially Stabilized Zirconia-Yttria, *Advances in Ceramics*, Vol 3, A.H. Heuer and L.W. Hobbs, Ed., American Ceramic Society, 1981, p 241-253
29. G.C. Chang and W. Phucharoen, Behavior of Thermal Barrier Coatings for Advanced Gas Turbine Blade, *Surf. Coat. Technol.*, Vol 30, 1987, p 13-28
30. G.C. Chang, W. Phucharoen, and R.A. Miller, Finite Element Thermal Stress Solutions for Thermal Barrier Coatings, *Surf. Coat. Technol.*, Vol 32, 1987, p 307-325
31. R.A. Cutler, J.R. Reynold, and A. Jones, Sintering and Characterization of Polycrystalline Monoclinic, Tetragonal, and Cubic Zirconia, *J. Am. Ceram. Soc.*, Vol 75 (No. 8), 1992, p 2173-2183
32. K.S. Shi, Z.Y. Qian, and M.S. Zhuang, Microstructure and Properties of Sprayed Ceramic Coating, *J. Am. Ceram. Soc.*, Vol 71 (No. 11), 1988, p 924-929
33. N.R. Shankar, C.C. Berndt, and H. Herman, Failure and Acoustic-Emission Response of Plasma-Sprayed  $ZrO_2$ -8wt% $Y_2O_3$  Coatings, *Ceram. Eng. Sci. Proc.*, Vol 3 (No. 9-10), 1982, p 772-792
34. C.C. Berndt and R.A. Miller, Mechanical Property Measurements of Plasma-Sprayed Thermal-Barrier Coatings Subjected to Oxidation, *Ceram. Eng. Sci. Proc.*, Vol 5 (No. 7-8), 1984, p 479-490